J. Phys. Chem. A **1998,** *102,* 1297−1303

Laser-Photolysis Studies of Isocyanide Complexes of Chlorochromium(III) Tetraphenylporphyrin in Toluene Solutions

Mikio Hoshino,* Takahiro Nagamori, Hiroshi Seki, Teiji Chihara, Takahiro Tase, and Yasuo Wakatsuki

The Institute of Physical and Chemical Research, Wako, Saitama 351-01, Japan

Masahiko Inamo

Faculty of Education, Aichi University of Education, Kariya, Aichi 448, Japan

Received: August 8, 1997; In Final Form: November 11, 1997

Chloroaquachromium(III) tetraphenylporphyrin, $Cl(H_2O)Cr^{III}TPP$, reversibly reacts with isocyanide, CN−R, to form $Cl(CN-R)Cr^{III}TPP$ in toluene solutions containing 4.4×10^{-3} M H_2O and CN−R. The equilibrium constant for the formation of $Cl(CN-R)Cr^{III}TPP$ obtained by spectroscopic measurements ranges from 10 to 10^2 depending on the nature of the isocyanide used. The laser-photolysis studies of the toluene solution demonstrate that CN−R is photodissociated from $Cl(CN-R)Cr^{III}TPP$ to produce $ClCr^{III}TPP$ with a quantum yield ca. 0.1. The five-coordinate $ClCr^{III}TPP$ reacts with H_2O and CN−R to give $Cl(H_2O)Cr^{III}TPP$ and $Cl(CN-R)Cr^{III}TPP$, respectively. The transient product $Cl(H_2O)Cr^{III}TPP$ further reacts with CN−R to regenerate $Cl(CN-R)Cr^{III}TPP$. The rates for the decay of $Cl(H_2O)Cr^{III}TPP$ are measured as a function of the concentration of CN−R in order to determine the rate constants of the forward and backward reactions for the formation of $Cl(CN-R)Cr^{III}TPP$. The equilibrium constants obtained from the kinetic analysis for the decay of $Cl(H_2O)Cr^{III}TPP$ are in good agreement with those determined by spectroscopic measurements. The mechanism for the equilibrium reaction is discussed in detail on the basis of the rate constants for the formation of $Cl(H_2O)Cr^{III}TPP$ and $Cl(CN-R)Cr^{III}TPP$ from $ClCr^{III}TPP$, measured in the temperature range 200−300 K. The quantum yield for the photodissociation of CN−R is not affected by the presence of oxygen. Since the lowest excited state $^6T_1$ of $Cl(CN-R)Cr^{III}TPP$ observed by laser photolysis is effectively quenched by oxygen, this state is not responsible for the ligand ejection from $Cl(CN-R)Cr^{III}TPP$. The $^4S_1$ state is assumed to be the reactive excited state of $Cl(CN-R)Cr^{III}TPP$.

Introduction

The excited states of chromium(III) porphyrins have been well studied both theoretically and experimentally.[1,2] According to the theoretical consideration,[1] the central chromium(III) atom[3] having a spin state $S = {}^3/_2$ interacts with the porphyrin π system in the excited states to give the $^4S_1$, $^2T_1$, $^4T_1$, $^6T_1$ states. The first one and the last three are, respectively, produced by a coupling of the central chromium atom ($S = {}^3/_2$) to the lowest excited singlet and the triplet state of the porphyrin π system.[1] The studies on the emission from the chromium(III) porphyrins have shown that the $^4T_1$ and $^6T_1$ states are in equilibrium because of the small energy difference between them.

The axial ligand significantly affects the electronic structure and the reactivity of metalloporphyrins in either the ground and excited states.[2] The laser-photolysis studies of chlorochromium(III) tetraphenylporphyrins, $Cl(L)Cr^{III}TPP$ (L = sixth axial ligand), have revealed that the yields for photodissociation of the axial ligands markedly depend on the nature of L.[4−7] For instance, $Cl(H_2O)Cr^{III}TPP$ photodissociates the axial H_2O with a quantum yield $\Phi = 0.98$,[7] while $Cl(CH_3COCH_3)Cr^{III}TPP$ photochemically releases the axial acetone with $\Phi = 0.15$.[4] The excited state responsible for the photodissociation of the sixth ligand is assumed to be the $^4S_1$ state of the chromium(III) porphyrin. Others, $^2T_1$, $^4T_1$, and $^6T_1$, are independent of the photodissociation of the axial ligands.[4−7]

$ClCr^{III}TPP$ synthesized has a water molecule at the axial position as revealed by X-ray structure determination.[6] The addition of isocyanide (CN−R) into a toluene solution of $Cl(H_2O)Cr^{III}TPP$ yields the isocyanide complexes $Cl(CN-R)Cr^{III}TPP$. The present paper describes the absorption spectroscopic and laser-photolysis studies of $Cl(CN-R)Cr^{III}TPP$ in toluene. The complex $Cl(CN-R)Cr^{III}TPP$ photodissociates CN−R by laser photolysis to yield the five-coordinate $ClCr^{III}TPP$. The reactive excited state for photodissociation and the association mechanisms of CN−R to both $Cl(H_2O)Cr^{III}TPP$ and the five-coordinate $ClCr^{III}TPP$ are discussed on the basis of the laser-photolysis studies carried out in the temperature range 300−200 K.

Experimental Section

Toluene was supplied from Wako Pure Chemicals Industry Ltd. The concentration of water in toluene used in the present study is 4.4×10^{-3} M. The isocyanides used were CN−R^n (n = 1−5; see Chart 1), which were synthesized according to literature.[8−10] Chloroaquachromium(III) tetraphenylporphyrin, $Cl(H_2O)Cr^{III}TPP$, was synthesized and purified by the method reported in ref 3. The concentration of $Cl(H_2O)Cr^{III}TPP$ in toluene is ca. 10^{-5} M during the course of this study. The sample quartz cells have an optical path length of 1 cm.

---

* To whom correspondence should be addressed. Telephone: 048-467-9426. Fax: 048-462-4668. E-mail: hoshino@postman.riken.go.jp.

S1089-5639(97)02590-5 CCC: $15.00

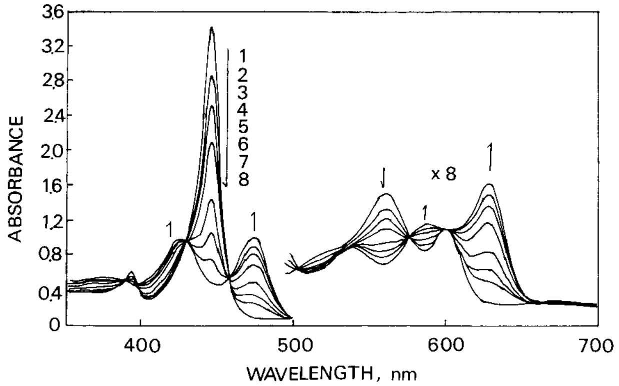

Figure 1. Absorption spectral changes observed for $Cl(H_2O)Cr^{III}TPP$ in a toluene solution containing 4.4×10^{-3} M H_2O and $CN-R^1$. The concentrations of $CN-R^1$ are (1) 0, (2) 1.11×10^{-5}, (3) 2.22×10^{-5}, (4) 4.44×10^{-5}, (5) 1.11×10^{-4}, (6) 2.22×10^{-4}, (7) 5.55×10^{-4}, and (8) 1.0×10^{-2} M.

CHART 1

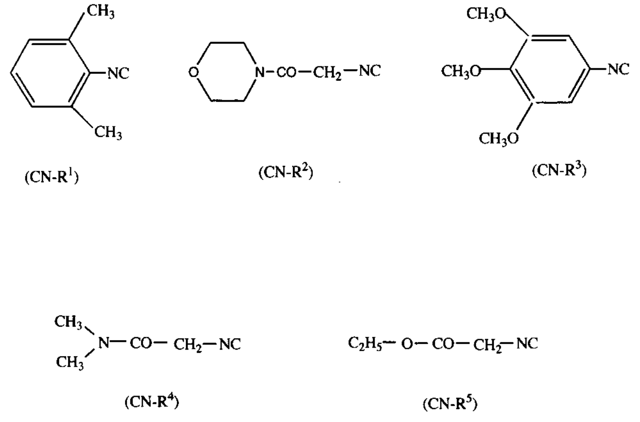

Absorption spectra were recorded on a Hitachi 330 spectrophotometer. Laser-photolysis studies were carried out with the use of a Nd:YAG laser equipped with the second (532 nm), third (355 nm), and fourth (266 nm) harmonic generators. The duration and the energy of a laser pulse at 355 nm were, respectively, 20 ns and 60 mJ/pulse. The detection system of the transient is described elsewhere.[11] The temperatures of the sample solutions were controlled with the use of an Oxford cryostat (model DN 1007).

Results

Absorption Spectroscopic Studies of Isocyanide Complexes. Figure 1 shows the absorption spectral changes observed for $Cl(H_2O)Cr^{III}TPP$ in the toluene solution with a change in the concentration of $CN-R^1$. The absorption peaks of $Cl(H_2O)Cr^{III}TPP$ located at 394, 448, and 562 nm decrease in intensity, and new peaks appear at 427, 474, 585, and 628 nm with an increase in the concentration of the $CN-R^1$. Clear isosbestic points observed in the spectra indicate that the spectral changes are interpreted in terms of the equilibrium reaction

$$Cl(H_2O)Cr^{III}TPP + CN-R^1 \underset{k_b}{\overset{k_f}{\rightleftharpoons}} Cl(CN-R^1)Cr^{III}TPP + H_2O \quad (1)$$

The equilibrium constant K ($=k_f/k_b$) is expressed as

$$K = \frac{[Cl(CN-R^1)Cr^{III}TPP][H_2O]}{[Cl(H_2O)Cr^{III}TPP][CN-R^1]} \quad (2)$$

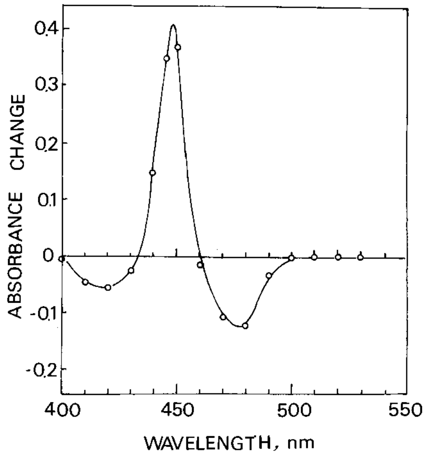

Figure 2. Transient absorption spectrum observed for the toluene solution of $Cl(CN-R^1)Cr^{III}TPP$ in the presence of 1.13×10^{-3} M $CN-R^1$ at 300 K. The spectrum was taken at 1.0 μs after 355-nm laser pulsing. The short-lived species completely disappeared within 1.0 μs after pulsing (data not shown).

Equation 3 is derived from eqs 1 and 2:

$$Y = \frac{(D - D_0)}{(D_\infty - D)} = K\frac{[CN-R^1]}{[H_2O]} \quad (3)$$

Here, D is the absorbance at $[CN-R^1]$, and D_0 and D_∞ stand for the absorbances at $[CN-R^1] = 0$ and at an "infinite" concentration of $CN-R^1$, respectively. The plot of Y vs $[CN-R^1]$ gives a straight line with an intercept at the origin. The slope of the line gives $K/[H_2O] = 2.9 \times 10^4$ M^{-1}. The concentration of water in toluene is 4.4×10^{-3} M, and thus, the equilibrium constant K is determined as 1.28×10^2.

The absorption spectrum of $Cl(CN-R^1)Cr^{III}TPP$ exhibits characteristic features particularly in the Soret band region. The absorption band of $Cl(H_2O)Cr^{III}TPP$ located at 448 nm splits into two bands with intensity similar to each other by forming the isocyanide complex, one at 427 and another at 474 nm. The molar absorption coefficients of $Cl(CN-R^1)Cr^{III}TPP$ in toluene are determined as 6.4×10^4 $M^{-1}cm^{-1}$ at 427 nm and 6.6×10^4 $M^{-1}cm^{-1}$ at 474 nm. These values are smaller than that (2.33×10^5 M^{-1} cm^{-1}) of $Cl(H_2O)Cr^{III}TPP$ at 448 nm. The spectra, the peak wavelengths, and the molar absorption coefficients obtained for the five isocyanide complexes in the Soret band region are very close each other, independent of the nature of the isocyanide studied.

Laser-Photolysis Studies. The laser-photolysis studies were carried out for the toluene solution of $Cl(H_2O)Cr^{III}TPP$ in the presence of 1.13×10^{-3} M $CN-R^1$ at 300 K. The major chromium porphyrin species (>99.9%) in the solution was confirmed to be $Cl(CN-R^1)Cr^{III}TPP$. The transient spectrum observed at 300 K shows that short- and long-lived species are produced; the former decays within 1.0 μs after pulsing and the latter over a few tens of microseconds. We initially describe the kinetic study of the long-lived species. The short-lived species will be mentioned later.

Figure 2 shows the long-lived transient absorption spectrum measured at 1.0 μs after pulsing. The transient spectrum has a positive peak at 448 nm and a negative one at 480 nm. The spectrum is in good agreement with the difference spectrum obtained by subtracting the spectrum of $Cl(CN-R_1)Cr^{III}TPP$ from that of $Cl(H_2O)Cr^{III}TPP$. Thus, the laser photolysis of $Cl(CN-R^1)Cr^{III}TPP$ is concluded to yield $Cl(H_2O)Cr^{III}TPP$. The decay of the transient $Cl(H_2O)Cr^{III}TPP$ strictly follows first-

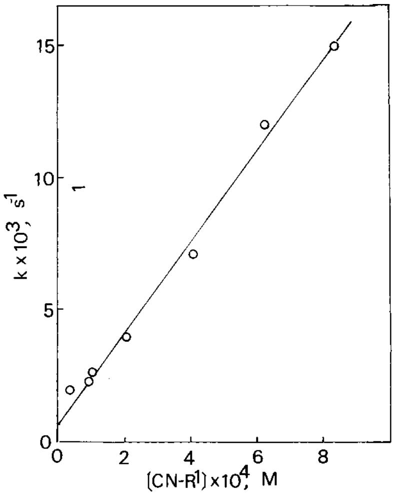

Figure 3. Plot of the rate constants k for the decay of $Cl(H_2O)Cr^{III}TPP$ represented as a function of the concentration of $CN-R^1$.

TABLE 1: Rate Constants k_f and k_b and Equilibrium Constants K for the Formation of $Cl(CN-R^n)Cr^{III}TPP$ from $Cl(H_2O)Cr^{III}TPP$ in Toluene[a]

	isocyanide				
	$CN-R^1$	$CN-R^2$	$CN-R^3$	$CN-R^4$	$CN-R^5$
k_f, $M^{-1}\,s^{-1}$	$1.7_5 \times 10^7$	1.7×10^7	1.6×10^7	1.6×10^7	1.8×10^7
k_b, $M^{-1}\,s^{-1}$	1.4×10^5	1.6×10^5	6×10^5	1.9×10^5	1.7×10^5
K	$1.2_5 \times 10^2$	1.1×10^2	2.7×10	8.5×10	1.1×10
$*k_f$ (calcd), $M^{-1}\,s^{-1}$	2.9×10^7	1.1×10^7	1.8×10^7	1.1×10^7	1.7×10^7
$*k_b$ (calcd), s^{-1}	2.3×10^5	1.0×10^5	6.6×10^5	1.2×10^5	1.6×10^5

[a] Experimental errors are within ±10%. $*k_f$ (calcd) and $*k_b$ (calcd) are the values of k_f and k_b calculated with eqs 18 and 19.

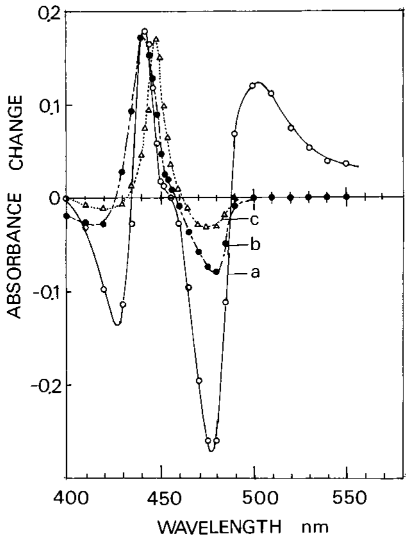

Figure 4. Transient absorption spectra observed for the toluene solution of $Cl(CN-R^1)Cr^{III}TPP$ in the presence of 1.13×10^{-3} M $CN-R^1$ at 210 K. The spectra were taken at (a) 50 ns, (b) 2.5 μs, and (c) 20 μs.

order kinetics. The decay rate constant, k, was measured as a function of the concentration of $CN-R^1$. Figure 3 shows the plot of k vs $[CN-R^1]$, which gives a straight line with an intercept. According to eq 1, the rate constant k is expressed as

$$k = k_f[CN-R^1] + k_b[H_2O] \qquad (4)$$

The slope and intercept of the line in Figure 3 give $k_f = 1.75 \times 10^7\ M^{-1}\,s^{-1}$ and $k_b[H_2O] = 6.2 \times 10^2\ s^{-1}$, respectively. From the latter value and $[H_2O] = 4.4 \times 10^{-3}$ M, k_b is determined as $1.40 \times 10^5\ M^{-1}\,s^{-1}$. The equilibrium constant K is calculated to be 1.25×10^2, in fairly good agreement with that obtained from the spectroscopic titration of $Cl(H_2O)Cr^{III}TPP$ with $CN-R^1$. In Table 1 are listed the values for k_f, k_b, and K obtained with $CN-R^n$.

It is noteworthy that, in contrast to the case of chlorocobalt(III)[12] and -Fe(III) porphyrins,[13] the axial Cl of $Cl(H_2O)Cr^{III}TPP$ and $Cl(CN-R^1)Cr^{III}TPP$ is not photodissociated.

As mentioned above, the laser photolysis of $Cl(CN-R^1)Cr^{III}TPP$ in the toluene solution at 300 K yields short-lived species with a lifetime shorter than 1 μs. To clearly detect the short-lived species, the laser photolysis of $Cl(CN-R^1)Cr^{III}TPP$ was carried out at the temperatures below 300 K. Figure 4 shows the transient spectra observed for the toluene solution of $Cl(CN-R^1)Cr^{III}TPP$ at 210 K after 355-nm laser pulsing. The transient spectrum detected at 50 ns has positive peaks at 442 and 498 nm and negative ones at 425 and 478 nm. At 2.5 μs after pulsing, the fast decay component disappears, leaving the second transient spectrum, which has a positive peak at 442 nm and negative ones at 415 and 478 nm. The second transient further changes to the third one at ca. 20 μs after pulsing. The third transient is readily ascribed to $Cl(H_2O)Cr^{III}TPP$ as observed by the laser photolysis of $Cl(CN-R^1)Cr^{III}TPP$ at 300 K. The second transient, which is a precursor of $Cl(H_2O)Cr^{III}TPP$, is considered to be the five-coordinate $ClCr^{III}TPP$. The transient spectrum taken at 50 ns after pulsing is interpreted as a sum of those of $Cl(CN-R^1)Cr^{III}TPP$ in the excited sextet state $^6T_1$ and the five-coordinate $ClCr^{III}TPP$. The sextet state of $Cl(CN-R^1)Cr^{III}TPP$ exhibits a positive peak around 500 nm[4-7] with a decay rate constant of $1.6 \times 10^6\ s^{-1}$ at 210 K. The photochemistry of $Cl(CN-R^1)Cr^{III}TPP$ in the toluene solution is summarized as

$$Cl(CN-R^1)Cr^{III}TPP + h\nu \rightarrow {}^6T_1 \qquad (5)$$

$$Cl(CN-R^1)Cr^{III}TPP + h\nu \rightarrow ClCr^{III}TPP + CN-R^1 \qquad (6)$$

$${}^6T_1 \xrightarrow{k_{(^6T_1)}} Cl(CN-R^1)Cr^{III}TPP \qquad (7)$$

$$ClCr^{III}TPP + CN-R^1 \xrightarrow{k_{(CN-R^1)}} Cl(CN-R^1)Cr^{III}TPP \qquad (8)$$

$$ClCr^{III}TPP + H_2O \xrightarrow{k_{(H_2O)}} Cl(H_2O)Cr^{III}TPP \qquad (9)$$

$Cl(CN-R^1)Cr^{III}TPP$ absorbs laser pulses to give the $^6T_1$ state and the five-coordinate $ClCr^{III}TPP$. The $^6T_1$ state returns to the ground $Cl(CN-R^1)Cr^{III}TPP$. The five-coordinate $ClCr^{III}TPP$ reacts with H_2O and $CN-R^1$ to yield $Cl(CN-R^1)Cr^{III}TPP$ and $Cl(H_2O)Cr^{III}TPP$, respectively. $Cl(H_2O)Cr^{III}TPP$ finally returns to $Cl(CN-R^1)Cr^{III}TPP$ according to eq 1. The results mentioned above leads to the conclusions that (1) the short-lived species detected at 300 K are ascribed to the $^6T_1$ state of $Cl(CN-R^1)Cr^{III}TPP$ and (2) the long-lived transient $Cl(H_2O)Cr^{III}TPP$ observed at 300 K is produced by the reaction of the five-coordinate $ClCr^{III}TPP$ and H_2O.

Equations 8 and 9 are the competitive processes, and thus, the yield of $Cl(H_2O)Cr^{III}TPP$ is expected to diminish with the increase in the concentration of $CN-R^1$. The relative yields Γ for the formation of $Cl(H_2O)Cr^{III}TPP$ at 300 K are obtained by measuring the 448-nm absorbance change ΔD(448 nm) at 1 μs after laser pulsing. Figure 5 shows the plot of ΔD(448 nm) vs

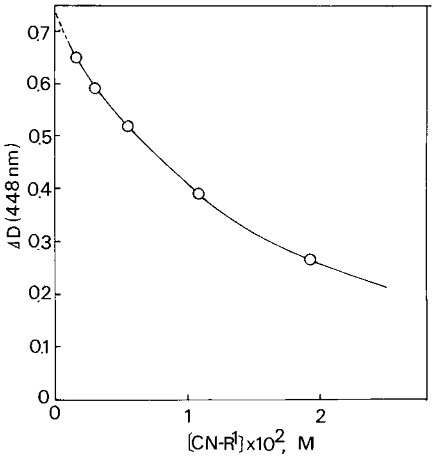

Figure 5. Plot of ΔD(448 nm) as a function of [CN−R^1] (see text).

[CN−R^1]. According to eqs 8 and 9, Γ is formulated as

$$\Gamma = \frac{\Delta D(448\ \text{nm})}{\Delta D_0(448\ \text{nm})} = \frac{k_{(H_2O)}[H_2O]}{k_{(H_2O)}[H_2O] + k_{(CN-R^1)}[CN-R^1]} \qquad (10)$$

where ΔD_0(448 nm) is the absorbance change at [CN−R^1] = 0. The plot of Γ^{-1} vs [CN−R^1] gives a straight line. From the slope of the line, the value of $k_{(CN-R^1)}/(k_{(H_2O)}[H_2O])$ at 300 K is obtained as 8.33 × 10 M^{-1}, and thus, $k_{(CN-R^1)}/k_{(H_2O)} = 0.366$ at 300 K. Since $k_{(H_2O)}$ has been determined to be 1.2 × 10^9 M^{-1}s^{-1},[6] $k_{(CN-R^1)}$ at 300 K is obtained as 4.4 × 10^8 M^{-1}s^{-1}.

Mechanism of Ligand Substitution. The ligand substitution reaction of coordination compounds is generally interpreted in terms of the S$_N$1 or the S$_N$2 type mechanism. On the assumption that the forward and backward reactions in eq 1 occur according to the S$_N$1 type mechanism, the equilibrium between Cl(H$_2$O)Cr^{III}TPP and Cl(CN−R^1)Cr^{III}TPP is expressed by

$$\text{Cl(H}_2\text{O)Cr}^{III}\text{TPP} \underset{k_{(H_2O)}}{\overset{k_{b(H_2O)}}{\rightleftharpoons}} \text{ClCr}^{III}\text{TPP} + \text{H}_2\text{O} \qquad (11)$$

$$\text{ClCr}^{III}\text{TPP} + \text{CN}-\text{R}^1 \underset{k_{b(CN-R^1)}}{\overset{k_{(CN-R^1)}}{\rightleftharpoons}} \text{ClCr}^{III}\text{TPP(CN}-\text{R}^1) \qquad (12)$$

Equations 11 and 12 lead to the following equation:

$$K = \frac{[\text{Cl(CN}-\text{R}^1)\text{Cr}^{III}\text{TPP}][\text{H}_2\text{O}]}{[\text{Cl(H}_2\text{O)Cr}^{III}\text{TPP}][\text{CN}-\text{R}^1]} = \frac{k_{(CN-R^1)}}{k_{b(CN-R^1)}}\,\frac{k_b(H_2O)}{k_{(H_2O)}} \qquad (13)$$

With the use of $K = 1.25 \times 10^2$, $k_{b(H_2O)} = 3.5 \times 10^5$ s^{-1},[6] $k_{(H_2O)} = 1.2 \times 10^9$ M^{-1} s^{-1},[6] and $k_{(CN-R^1)} = 4.4 \times 10^8$ M^{-1} s^{-1}, we obtain $k_{b(CN-R^1)} = 1.0 \times 10^3$ s^{-1}. The equilibrium constant, $K_{(CN-R^1)} = k_{(CN-R^1)}/k_{b(CN-R^1)}$, in eq 12 is obtained as 4.4 × 10^5. In Table 2 are listed the values $k_{(CN-R^n)}$, $k_{b(CN-R^n)}$, and the equilibrium constant $K_{(CN-R^n)}$ for all CN−R^n studied.

TABLE 2: Rate Constants $k_{(CN-R^n)}$ and $k_{b(CN-R^n)}$ and the Equilibrium Constants $K_{(CN-R^n)}$ for the Formation of Cl(CN−R^n)Cr^{III}TPP from ClCr^{III}TPP, and the Quantum Yields Φ for the Photodissociation of CN−R^n from Cl(CN−R^n)Cr^{III}TPP[a]

	isocyanide				
	CN−R^1	CN−R^2	CN−R^3	CN−R^4	CN−R^5
$k_{(CN-R^n)}$, M^{-1} s^{-1}	4.4 × 10^8	1.7 × 10^8	2.7 × 10^8	1.6$_6$ × 10^8	2.6 × 10^8
$k_{b(CN-R^n)}$, s^{-1}	1.0 × 10^3	4.7 × 10^2	2.9$_5$ × 10^3	2.9 × 10^2	6.9 × 10^2
$K_{(CN-R^n)}$	4.4 × 10^5	3.6 × 10^3	9.2$_5$ × 10^4	2.9 × 10^5	3.8 × 10^5
Φ	0.09$_4$	0.11	0.10	0.10	0.09$_8$

[a] Experimental errors are within ±10%. The quantum yields Φ were found to be independent of the laser energy in the range 20−60 mJ/pulse.

From eqs 11 and 12, the rate constant k for achieving the equilibrium reaction (eq 1) can be obtained with the use of the steady-state approximation with regard to ClCr^{III}TPP:

$$d[\text{ClCr}^{III}\text{TPP}]/dt = 0 \qquad (14)$$

$$[\text{ClCr}^{III}\text{TPP}] \ll [\text{Cl(CN}-\text{R}^1)\text{Cr}^{III}\text{TPP}] \text{ and } [\text{Cl(H}_2\text{O)Cr}^{III}\text{TPP}] \qquad (15)$$

Equations 11, 12, 14, and 15 give the expression for k as follows.

$$k = \frac{k_{b(H_2O)}k_{(CN-R^1)}[CN-R^1] + k_{(H_2O)}k_{b(CN-R^1)}[H_2O]}{k_{(H_2O)}[H_2O] + k_{(CN-R^1)}[CN-R^1]} \qquad (16)$$

Since $k_{(H_2O)}[H_2O] \gg k_{(CN-R^1)}[CN-R^1]$ holds in the present system ([CN−R^1] < 10^{-3} M), eq 16 is transformed to eq 17:

$$k = \{k_{b(H_2O)}k_{(CN-R^1)}[CN-R^1]\}\{k_{(H_2O)}[H_2O]\}^{-1} + k_{b(CN-R^1)} \qquad (17)$$

From eqs 4 and 17, k_f and k_b are, respectively, represented as

$$k_f = \{k_{b(H_2O)}k_{(CN-R^1)}\}\{k_{(H_2O)}[H_2O]\}^{-1} \qquad (18)$$

$$k_b = k_{b(CN-R^1)}[H_2O]^{-1} \qquad (19)$$

Thus, when the equilibrium reaction in eq 1 proceeds via an intermediate ClCr^{III}TPP, k_f and k_b will be given by eqs 18 and 19, respectively. In Table 1 are listed the $^*k_f$ and $^*k_b$ values, which are calculated for CN−R^n according to eqs 18 and 19 with the use of $k_{b(H_2O)}$, $k_{(H_2O)}$, $k_{(CN-R^1)}$, $k_{b(CN-R^1)}$, and [H$_2$O]. It is found from Table 1 that the values of k_f and k_b experimentally obtained are moderately in good agreement with those of $^*k_f$ and $^*k_b$ calculated. This finding suggests that the ligand-substitution reaction in eq 1 occurs through the S$_N$1-type mechanism; i.e., the five-coordinate ClCr^{III}TPP is a key intermediate in eq 1.

Temperature Dependence of Rate Constants. From eqs 8 and 9, the rate constant $k_d(T)$ for the decay of ClCr^{III}TPP at a temperature T is given by

$$k_d(T) = k_{(CN-R^1)}(T)[CN-R^1] + k_{(H_2O)}(T)[H_2O] \qquad (20)$$

The value of $k_d(T)$ was measured in the temperature range 200−300 K. $k_d(T)$ was found to decrease with a decrease in temperature. Thus, the associations of CN−R^1 and H$_2$O to ClCr^{III}TPP are expected to be activation processes. The two terms $k_{(CN-R^1)}(T)$ and $k_{(H_2O)}(T)$ in eq 20 at various temperatures are separately obtained by measuring both $k_d(T)$ and the relative

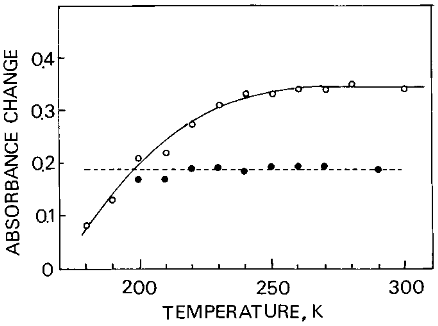

Figure 6. Plots of the absorbance changes ΔD_0(448 nm, T) (○) and ΔD_0(433 nm, T) (●) as a function of temperature.

quantum yields for the photochemical formation of $ClCr^{III}TPP$ and $Cl(H_2O)Cr^{III}TPP$ from $Cl(CN{-}R^1)Cr^{III}TPP$ in the toluene solution as a function of T.

Figure 6 shows the plots of ΔD_0(448 nm, T) and ΔD_0(433 nm, T) observed at a temperature T for a toluene solution of $Cl(CN{-}R^1)Cr^{III}TPP$ in the presence of 1.13×10^{-3} M $CN{-}R^1$, represented as a function of temperature. Here, ΔD_0(433 nm, T) was measured at 433 nm immediately after the $^6T_1$ state of $Cl(CN{-}R^1)Cr^{III}TPP$ disappeared. The values of ΔD_0(448 nm,T) and ΔD_0(433 nm,T) are, respectively, the relative yields for the formation of $Cl(H_2O)Cr^{III}TPP$ and $ClCr^{III}TPP$. As shown in Figure 6, ΔD_0(433 nm, T) is 0.18 ± 0.1 in the temperature range 200−300 K. Therefore, the quantum yield for the photodissociation of $CN{-}R^1$ from $Cl(CN{-}R^1)Cr^{III}TPP$ is concluded to be independent of temperature in the range studied. However, ΔD_0(448 nm, T) shows a temperature dependence: the yield for the formation of $Cl(H_2O)Cr^{III}TPP$ increases with an increase in temperature and levels off above 260 K to give a value of $\Delta D_0(448\text{ nm}, \infty) = 0.35$. These results indicate that the observed low yields of $Cl(H_2O)Cr^{III}TPP$ at low temperatures are ascribed to the decrease in $k_{(H_2O)}(T)$. On the basis of the results mentioned above and eqs 8 and 9, the relative yield $\phi_r(T)$ for the formation of $Cl(H_2O)Cr^{III}TPP$ is represented as

$$\begin{aligned}\phi_r(T) &= \Delta D_0(448\text{ nm}, T)/\Delta D_0(448\text{ nm}, 300\text{ K})\\ &= (\Gamma)^{-1}k_{(H_2O)}(T)[H_2O]\{k_{(CN-R^1)}(T)[CN{-}R^1] +\\ &\qquad k_{(H_2O)}(T)[H_2O]\}^{-1} \quad (21)\end{aligned}$$

Here, $\phi_r(T) = 1.0$ at 300 K, and thus, the Γ value in the present system ($[CN{-}R^1] = 1.13 \times 10^{-3}$ M and $[H_2O] = 4.4 \times 10^{-3}$ M) is calculated to be 0.91 from eq 10. Equations 20 and 21 lead to

$$k_{(H_2O)}(T) = k_d(T)\Gamma\phi_r(T)/[H_2O] \qquad (22)$$

$$k_{(CN-R^1)}(T) = k_d(T)\{1 - \Gamma\phi_r(T)\}/[CN{-}R^1] \qquad (23)$$

By use of $[H_2O] = 4.4 \times 10^{-3}$ M, $[CN{-}R^1] = 1.13 \times 10^{-3}$ M, $k_d(T)$, and $\phi_r(T)$, the values of $k_{(H_2O)}(T)$ and $k_{(CN-R^1)}(T)$ are obtained at various temperatures.

Figure 7 shows $k_{(H_2O)}(T)$ and $k_{(CN-R^1)}(T)$ represented as a function of temperature. The plots of $\log k_{(H_2O)}(T)$ and $\log k_{(CN-R^1)}(T)$ vs $1/T$ gave straight lines. The Arrhenius expressions for $k_{(H_2O)}(T)$ and $k_{(CN-R^1)}(T)$ are

$$k_{(H_2O)}(T) = 1.7 \times 10^{14} \exp\left(-\frac{7.0 \times 10^3}{RT}\right) \text{M}^{-1}\text{ s}^{-1} \qquad (24)$$

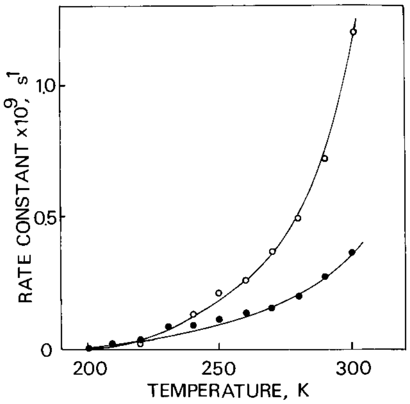

Figure 7. Rate constants $k_{(H_2O)}(T)$ (○) and $k_{(CN-R^1)}(T)$ (●) as a function of temperature.

$$k_{(CN-R^1)}(T) = 4.0 \times 10^{11} \exp\left(-\frac{4.1 \times 10^3}{RT}\right) \text{M}^{-1}\text{ s}^{-1} \qquad (25)$$

The relative yield for the formation of the $^6T_1$ state of $Cl(CN{-}R^1)Cr^{III}TPP$ was measured in the temperature range 180−300 K by monitoring the absorbance change at 500 nm after laser pulsing. The yield exhibited a slight increase below 190 K.

Quantum-Yield Measurements. Quantum yields Φ for the formation of $Cl(H_2O)Cr^{III}TPP$ from $Cl(CN{-}R^1)Cr^{III}TPP$ were measured at room temperature by the laser-photolysis method described earlier.[14] The absorbance change ΔD_0(448 nm) is shown by

$$\Delta D_0(448\text{ nm}) = I_{abs}\Delta\epsilon_{AB}\Phi/N_A \qquad (26)$$

Here, I_{abs} is the number of 355-nm photons absorbed by a toluene solution of $Cl(CN{-}R^1)Cr^{III}TPP$ upon laser photolysis, $\Delta\epsilon_{AB}$ is the difference in the molar absorption coefficients at 448 nm between $Cl(CN{-}R^1)Cr^{III}TPP$ and $Cl(H_2O)Cr^{III}TPP$, and N_A is the Avogadro number. For determination of I_{abs}, a benzene solution of benzophenone, which is prepared to have the same absorbance at 355 nm as that of the toluene solution of $Cl(CN{-}R^1)Cr^{III}TPP$, was used; the molar absorption coefficient ϵ_T and the yield Φ_T of the triplet benzophenone have already been determined as 7.8×10^3 $\text{M}^{-1}\text{ cm}^{-1}$ at 530 nm and 1.0, respectively.[15,16] The absorbance of the triplet benzophenone, ΔD_T(530 nm) observed after 355-nm laser pulsing, is expressed as

$$\Delta D_T(530\text{ nm}) = I_{abs}\epsilon_T\Phi_T/N_A \qquad (27)$$

From eqs 26 and 27, eq 28 is derived:

$$\Phi = \Phi_T\frac{\epsilon_T}{\Delta\epsilon_{AB}}\frac{\Delta D_0(448\text{ nm})}{\Delta D_T(530\text{ nm})} \qquad (28)$$

The quantum yield for the formation of $Cl(H_2O)Cr^{III}TPP$ by laser photolysis of $Cl(CN{-}R^1)Cr^{III}TPP$ in toluene containing 1.13×10^{-3} M $CN{-}R^1$ and 4.4×10^{-3} M H_2O is obtained as 0.086 at 300 K. As mentioned above, $Cl(H_2O)Cr^{III}TPP$ is produced by the reaction of $ClCr^{III}TPP$ with H_2O in toluene. Thus, the yield $\Phi(ClCr^{III}TPP)$ for the formation of $ClCr^{III}TPP$ is represented by

$$\Phi(ClCr^{III}TPP) = \Phi\frac{k_{(CN-R^1)}[CN{-}R^1] + k_{(H_2O)}[H_2O]}{k_{(H_2O)}[H_2O]} \qquad (29)$$

The value of $\Phi(ClCr^{III}TPP)$ at 300 K is determined as 0.094

SCHEME 1

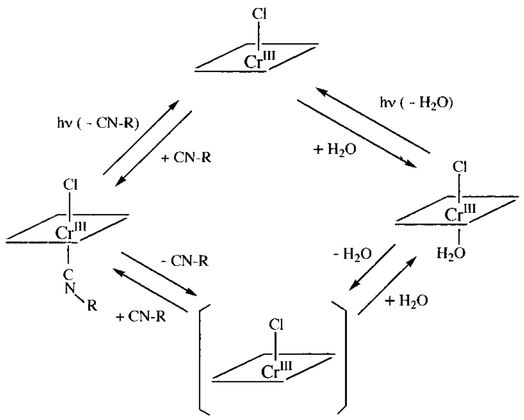

from eq 29. In Table 2 are listed the quantum yields for the formation of ClCr^{III}TPP from five isocyanide complexes of ClCr^{III}TPP in toluene at 300 K.

Discussion

A number of isocyanide complexes have been synthesized and characterized in order to elucidate the nature of the bonding between metal and isocyanides.[17] For metalloporphyrins, isocyanide complexes of iron[18−21] and rhodium porphyrins[22,23] have been well studied; the crystallographic structures of these complex are the bis[isocyanide] complexes.[19,20,22] The present study revealed that chromium(III) tetraphenylporphyrin forms a 1:1 complex with isocyanide in toluene solutions.

The equilibrium constants for the formation of Cl(CN−R^n)Cr^{III}TPP from Cl(H_2O)Cr^{III}TPP are found to be ranged from 10 to 10^2.

The laser-photolysis studies of Cl(CN−R^1)Cr^{III}TPP in the toluene solution containing 4.4×10^{-3} M H_2O demonstrate that the axial CN−R^1 is photodissociated to give five-coordinate ClCr^{III}TPP, which reacts with both H_2O and CN−R^1 to yield Cl(H_2O)Cr^{III}TPP and Cl(CN−R^1)Cr^{III}TPP, respectively. The detection of Cl(H_2O)Cr^{III}TPP as a transient indicates that the rate for the association of H_2O to ClCr^{III}TPP is faster than that of CN−R^1 in this solution at 300 K. The transient Cl(H_2O)Cr^{III}TPP further reacts with CN−R^1 to regenerate Cl(CN−R^1)Cr^{III}TPP. The rate constant for association of H_2O to ClCr^{III}TPP has been determined as 1.2×10^9 M^{-1} s^{-1},[6] and those of CN−R^n are $(1.7-5.3) \times 10^8$ M^{-1} s^{-1}.

Cl(H_2O)Cr^{III}TPP and Cl(CN−R^n)Cr^{III}TPP are in equilibrium in the toluene solution containing CN−R^n. The equilibrium constant K depends on the nature of CN−R^n. According to the laser-photolysis studies, the transient product ClCr^{III}TPP initially attains the equilibria shown by eqs 11 and 12. Since the rates for the dissociation of H_2O and CN−R^n in eqs 11 and 12 are very slow, ClCr^{III}TPP disappears to generates either Cl(H_2O)Cr^{III}TPP or Cl(CN−R^n)Cr^{III}TPP. Then Cl(H_2O)Cr^{III}TPP relaxes toward the equilibrium given by eq 1. The forward rate constants in eq 1 are almost identical: $(1.6-1.8) \times 10^7$ M^{-1} s^{-1} for all isocyanide complexes used. However, the backward rate constants in eq 1 vary from 10^5 to 10^6 M^{-1} s^{-1}.

The ligand-substitution reactions of Cl(L)Cr^{III}TPP (L: axial ligand) have been interpreted on the assumption that the reactions proceed via a five-coordinate intermediate ClCr^{III}TPP.[4,6] The detailed kinetic analysis of the present system also suggests that ClCr^{III}TPP is a key intermediate in eq 1. The reaction mechanism of the present system is displayed in Scheme 1.

The rate constants for the association of H_2O and CN−R^1 toward ClCr^{III}TPP were measured by laser photolysis of the toluene solution of Cl(CN−R^1)Cr^{III}TPP in the temperature range 300−200 K. The activation energy and preexponential factor obtained for the association of H_2O toward ClCr^{III}TPP are markedly larger than those expected from the diffusion process; the former is 1.7×10^{14} M^{-1} s^{-1} and the latter 7 kcal mol^{-1}. In an earlier paper, we have studied the photochemistry of Cl(H_2O)Cr^{III}TPP in a polystyrene film. The laser photolysis of Cl(H_2O)Cr^{III}TPP in the film results in the dissociation of the axial H_2O to produce ClCr^{III}TPP. The bimolecular rate constant for the recombination reaction between H_2O and ClCr^{III}TPP measured in the temperature range 200−300 K gives a preexponential factor of 10^{15} M^{-1} s^{-1} and an activation energy of 7 kcal mol^{-1}. Fairly large preexponential factors obtained for toluene solutions and polystyrene films suggest that water molecules in a hydrophobic solvent are able to move around more quickly than in a diffusion process. The activation energy obtained with toluene solutions is close to that with polystyrene films. Probably the reaction between ClCr^{III}TPP and H_2O in toluene proceeds via the same activation complex as that in polystyrene film. The frequency factor and activation energy obtained with the reaction of ClCr^{III}TPP and CN−R^1 can be explained by assuming the diffusion process.

The quantum yields for formation of Cl(H_2O)Cr^{III}TPP from Cl(CN−R^n)Cr^{III}TPP in toluene containing 4.4×10^{-3} M water and ca. 10^{-3} M CN−R^n are determined as ca. 0.1 at 300 K. Since ClCr^{III}TPP produced from photolysis of (CN−R^n)Cr^{III}TPP mostly reacts with H_2O to produce Cl(H_2O)Cr^{III}TPP in the toluene solutions, the yields for photodissociation of CN−R^n from the isocyanide complexes are calculated as ca. 0.1. These values are smaller than those of the photodissociation yields of the axial ligands from other six-coordinate chlorochromium(III) porphyrins.[4,6]

Photoinduced dissociation of axial ligands have been investigated for Cl(H_2O)Cr^{III}TPP,[6,7] Cl(Py)Cr^{III}TPP,[6,7] Cl(CH_3COCH_3)Cr^{III}TPP,[4] and ONO−Cr^{III}TPP.[5] The reactions are found to occur from the $^4S_1$ state. The long-lived excited state $^6T_1$ is not responsible for photodissociation of the axial ligands.[4−7] The laser photolysis of Cl(CN−R^1)Cr^{III}TPP in toluene also gives rise to the formation of the $^6T_1$ state. The lifetimes τ of the $^6T_1$ state are 280 ns in degassed toluene and $\tau < 70$ ns in oxygen-saturated toluene at 1 atm. It is clear that the $^6T_1$ state is quenched by oxygen. However, the yield for the formation of ClCr^{III}TPP and Cl(H_2O)Cr^{III}TPP from Cl(CN−R^1)Cr^{III}TPP in the degassed solution is identical with that in the oxygen-saturated solution. This finding indicates that, like other chromium porphyrins,[4−7] the $^6T_1$ state is not a reactive state, and the $^4S_1$ state would be responsible for the photodissociation of CN−R^1 from Cl(CN−R^n)Cr^{III}TPP. The quantum yield (ca. 0.1) for the photodissociation of CN−R^n from Cl(CN−R^n)Cr^{III}TPP is independent of temperature in the range 300−200 K. Thus, the dissociation of CN−R^1 from the reactive excited state is concluded to occur without any activation energy in the temperature range 200−300 K.

References and Notes

(1) Gouterman, M.; Hanson, L. K.; Khalil, G. E.; Leenstra, W. R,; Buchler, J. W. *J. Chem. Phys.* **1975**, *62*, 2343−2353.

(2) Gouterman, M. In *The Porphyrins*; Dolphin, D., Ed.; Academic Press: New York, 1978; Vol. III, Chapter 1.

(3) Summmerville, D. A.; Jones, R. D.; Hoffman, B. M.; Basolo, F. *J. Am. Chem. Soc.* **1977**, *99*, 8195−8202.

(4) Yamaji, M.; Hama, Y.; Hoshino, M. *Chem. Phys. Lett.* **1990**, *165*, 309−314.

(5) Yamaji, M.; Hama, Y.; Miyazaki, Y.; Hoshino, M. *Inorg. Chem*. **1992**, *31*, 932−934.

(6) Inamo, M.; Hoshino, M.; Nakajima, K.; Aizawa, S.; Funabashi, S. *Bull. Chem. Soc. Jpn*. **1995**, *68*, 2293−2303.

(7) Hoshino, M.; Tezuka, N.; Inamo, M. *J. Phys. Chem*. **1996**, *100*, 627−632.

(8) Hartman, G. D.; Weinstock, L. M. *Org. Synth.* **1988**, *VI*, 620−624.

(9) Obrecht, R.; Herrman, R.; Ugi, I. *Synthesis* **1985**, 400−402.

(10) Ozaki, Y.; Matsumoto, K.; Miyoshi, M. *Agric. Biol. Chem*. **1978**, *42*, 1565−1569.

(11) Hoshino, M.; Imamura, M.; Watanabe, S.; Hama, Y. *J. Phys. Chem*. **1984**, *88*, 45−49.

(12) Hoshino, M.; Kogure, M.; Amano, K.; Hinohara, T. *J. Phys. Chem*. **1989**, *93*, 6655−6659.

(13) Hendrickson, D. N.; Kinnard, M. G.; Suslick, K. S. *J. Am. Chem. Soc*. **1987**, *109*, 1243−1244.

(14) Hoshino, M.; Konishi, R.; Tezuka, N.; Ueno, I.; Seki, H. *J. Phys. Chem*. **1996**, *100*, 13569−13574.

(15) Bensasson, R.; Land, E. J. *Trans. Faraday Soc.* **1971**, *67*, 1904−1915.

(16) Hoshino, M.; Shizuka, H. In *Radiation Curing in Polymer Science and Technology*; Fouassier, J. P., Rabek, J. F., Eds.; Elsevier Science Publishers: London, 1993; Vol. II, Chapter 15.

(17) Singleton, E.; Oosthuizen, H. E. In *Advances in Organometallic Chemistry*; Stone, F. G. A., West, R., Eds.; Academic Press: New York, 1983; Vol. XXII, pp 209−310.

(18) Simonneaux, G.; Hindre, F.; Plouzennec, M. L. *Inorg. Chem*. **1989**, *28*, 823−825.

(19) Walker, F. A.; Nasri, H.; Turowska-Tyrk, I.; Mohanrao, K.; Watson, C. T.; Shokhirev, N. V.; Debrunner, P. G.; Scheit, W. R. *J. Am. Chem. Soc*. **1996**, *118*, 12109−12118.

(20) Jameson, G. B.; Ibers, J. A. *Inorg. Chem*. **1979**, *18*, 1200−1208.

(21) Plouzennec, M. L.; Bondon, A.; Sodano, P.; Simonneaux, G. *Inorg. Chem*. **1986**, *25*, 1254−1257.

(22) Boschi, T.; Licoccia, S.; Paolesse, R.; Tagliatesta, P. *Organometallics* **1989**, *8*, 330−336.

(23) Poszmik, G.; Carroll, P. J.; Wayland, B. B. *Organometallics* **1993**, *12*, 3410−3417.